Thermal and Photoreactivity of TiO_2 at the Gas−Solid Interface with Aliphatic and Aromatic Aldehydes

Charles A. Jenkins and Damien M. Murphy*

National ENDOR Centre, Department of Chemistry, Cardiff University, P.O. Box 912, Cardiff, CF1 3TB, U.K.

Received: June 18, 1998; In Final Form: October 21, 1998

EPR spectroscopy has been used to characterize the interactions between aldehydes and the surface of rutile TiO_2 active toward heterogeneous charge transfer and ultimately the formation of surface peroxyacyl radicals. Paramagnetic centers formed by vacuum reduction and UV irradiation of TiO_2 have been detected and characterized at the dehydroxylated particle surface. In low-temperature (100 K) gas−solid studies, reduced TiO_2 surfaces have been used as model systems for interfacial charge-transfer processes. Radical products resulting from aldehyde reduction are not detected at 100 K on the reduced surface even under UV irradiation. However, coadsorption of aldehydes with O_2 and subsequent UV irradiation on reduced TiO_2 surfaces does result in the formation of stable surface radicals at 100 K. When the reactions conditions are varied, such as aldehyde type and UV wavelength, these radicals were identified as peroxyacyl species ($RCO_3^{\bullet}$) stabilized at the semiconductor surface. The $RCO_3^{\bullet}$ radicals were only formed in coadsorption experiments and decayed irreversibly at $T > 250$ K. The results clearly demonstrate that the TiO_2 surface can participate in both the initiation and propagation stages of aldehyde photooxidation. Similar radical species were not detected in UV-irradiated TiO_2−aldehyde suspensions at 100 K.

Introduction

Titanium dioxide is an n-type photoactive semiconductor that exhibits high corrosion resistance, low toxicity, and efficient photocatalytic conversion rates in contact with both liquid and gas phases. It is widely used as a photostabilizing white pigment in aldehyde-containing coating systems (where UV-induced coating degradation can be problematic) and has been proposed as a suitable photocatalyst for a diverse range of applications, including remediation of marine oil pollution,[1] antitumor therapy,[2] and the detoxification of indoor atmospheres in urban environments.[3] An understanding of interfacial photochemistry at the molecular level, particularly the fundamental chemistry of electron transfer,[4] is thus considered central to the design of suitable photocatalysts.

In recent years, catalysis over TiO_2 powders and single crystals has been the subject of numerous investigations using a variety of theoretical and experimental methods. At temperatures exceeding 200 K, the TiO_2 surface is known to participate in thermal and dissociative catalytic pathways. In particular, the adsorption of aldehydes onto TiO_2 at temperatures exceeding 240 K is believed to result in the formation of dioxyalkylene species via the transfer of nucleophilic lattice oxygens from the oxide surface to the adsorbed substrate.[5] Reduced surfaces are known to increase the proportion of aldehydes adsorbing in the bidentate mode,[6] whereas monodentate binding is favored on the fully oxidized surface.[7] The reduced surface also contains a higher number of intrinsic defects, such as oxygen vacancies, which result in stronger attachment of oxygen-containing molecules and enhanced rates of dissociative chemisorption. Recently, Bates et al.,[8] using density functional calculations, have predicted that the adsorption behavior of methanol and water over stoichiometric TiO_2 surfaces is highly sensitive to reactant surface coverage. At 600 K, the ratio of dissociative to molecular methanol adsorption varied as a function of adsorbate conformation, which in turn was governed by the magnitude of intermolecular forces between adsorbates.[8]

In addition to thermally driven mass transfer at the TiO_2−substrate interface, the oxide surface also participates in photoinitiated atom and charge-transfer processes via the agency of charge carrier trapping centers. Many of these centers, including active species produced at the TiO_2 surface, are paramagnetic and have been characterized previously by many authors using EPR spectroscopy.[9−15] Deviations from stoichiometry by heating TiO_2 in vacuo were first reported by Gray et al.[16] in 1959 and were later attributed to conduction electrons trapped at defect centers forming EPR-active Ti^{3+} species.[17] Ti^{3+} centers, together with the paramagnetic trapped hole species O^-, can also be formed under UV irradiation. Such species are known to be catalytically active and have been the subject of many recent EPR studies with a view to determining their precise catalytic role.[18] EPR−photocatalysis studies using frozen colloidal suspensions are commonplace, often employing very low temperatures and high-power pulsed laser irradiation techniques.[13,14] Although the use of such methods has been successful in characterizing various stable trapped charge carrier centers at low temperatures, the EPR spectra of the observed organic species often display little evidence of surface radical character.

To detect radical formation at heterogeneous gas−solid interfaces, many techniques have been developed including matrix isolation from reactor gas streams and low temperature studies (4 K) of the interface. The former method has been successfully used to detect organic radicals (such as acyl and acyloxyl species) desorbing from catalyst surfaces, but suffers from the drawback that the EPR spectra of the matrix isolated species may contain little information regarding radical identity.[19] Direct EPR detection of surface-bound radical ions on

* Author for correspondence (email: sacdmm@cardiff.ac.uk).

10.1021/jp982690n CCC: $18.00
Published on Web 01/23/1999

TiO_2 has been successful for simple inorganic species such as SO_2 and O_2.[20] However, the direct detection of adsorbed organic radicals has met with limited success and is confined mainly to the study of radical anions and cations formed from the adsorption of organic molecules possessing extended π bonds or those containing an essentially "inorganic" functional group, e.g., perylene, TCNE, and *p*-nitrobenzene.[21] Although such species can be used to monitor charge transfer between the photocatalyst surface and adsorbed substrates, the radical species detected do not necessarily arise in catalytic processes of industrial or environmental significance.

In the present work, we provide evidence for the EPR characterization of several neutral surface peroxyacyl species (general formula $RCO_3^{\bullet}$), which are well-known oxidative intermediates in the initiated gas-phase oxidation of aldehydes.[22] The $RCO_3^{\bullet}$ radical is also known to participate in the formation of the respiratory irritant peroxyacyl nitrate, which can accumulate to dangerously high levels in photochemical smogs.[23] Indoor sources of volatile aldehydes include cigarette smoke and slow release from some furnishing materials.[24] The surface radical species were generated by UV irradiation of rutile TiO_2 containing coadsorbed molecular oxygen and selected aldehydes. The utility of the coadsorption method, as opposed to preadsorption, is demonstrated to be a key experimental feature in obtaining a successful model reaction system for photocatalytic oxidation processes, since the nature of the radical formed depends entirely on how the surface is pretreated with reactants. Indeed, the paucity of EPR data in the current literature, pertaining to the interaction of nonresonance stabilized organic adsorbates with TiO_2, may be partly due to the failure of preadsorption methods to provide evidence for surface radical species. Although it is recognized that the dehydroxylated TiO_2 surface employed in this study is not a truly representative model for aqueous oxidation processes, it undoubtedly provides a valuable means for the study of nonaqueous and gas-phase photocatalytic processes.

Experimental Section

The rutile TiO_2 material used throughout this work was supplied by ICI, Tioxide UK (surface area of 97 $m^2\ g^{-1}$). Prior to reaction with organic molecules, the polycrystalline TiO_2 powder was slowly heated under vacuum (10^{-5} Torr) at different temperatures (ca. 1 h at 723, 773, 823, 923, and 973 K). The thermally reduced material, in a vacuum-sealed EPR tube, was cooled to 77 K in liquid nitrogen before exposure to probe gases at this temperature. The aldehyde-to-O_2 ratio was 5:1 in the coadsorption experiments. The sample cell was then quickly transferred to the EPR cavity (precooled to 77 K), and the temperature was raised slowly to 100 K for subsequent in situ UV irradiations at this temperature. The high-purity O_2 gas was supplied by BOC Ltd. The aldehydes (paraformaldehyde, acetaldehyde, and benzaldehyde), of analytic grade, were supplied by Aldrich Chemicals Ltd.

A 1000 W Oriel Instruments UV lamp, incorporating a Hg−Xe arc lamp (250 nm to >2500 nm), was used for all irradiations in the presence of a water filter. The UV output below 280 nm accounts for only 4−5% of the total lamp output. The EPR spectra were recorded either on a Varian E-109 spectrometer or a Bruker ESP 300E series spectrometer. All spectra were recorded at X-band frequencies, 100 kHz field modulation, 10 mW power, and 100 K.

Results

Reduction of Rutile TiO_2 in Vacuo. To obtain the optimum concentration of surface Ti^{3+} centers (with a minimum concentration of interfering bulk species) for reaction with adsorbates, it was necessary to know the ratio of surface-to-bulk Ti^{3+} acquired at various reduction temperatures. This was carried out by reducing the TiO_2 sample for 1 h in vacuo in the temperature range 723−973 K. The resulting EPR spectra (not shown for brevity) are dominated by the presence of a Ti^{3+} signal and a minor signal at $g = 2.0023$, which arises from medium-polarized conduction electrons.[21] The thermally reduced sample was then exposed to O_2 (10 Torr) at 300 K for 10 s. The excess gaseous O_2 was then pumped off at this temperature. This results in reoxidation of surface Ti^{3+} centers to Ti^{4+} via electron transfer to adsorbed O_2 (forming the well-known adsorbed superoxide O_2^- anion) so that only a bulk Ti^{3+} remnant EPR signal remained. The sample was then heated to 500 K under dynamic vacuum, a temperature sufficiently high to destroy the adsorbed superoxide but too low to generate new Ti^{3+} centers. In this way, the signal intensities of the Ti^{3+} centers before and after thermal reduction could be compared. The results of this investigation are presented in Figure 1. It can be clearly seen that the ratio of surface-to-bulk Ti^{3+} cations decreases as the temperature is increased.

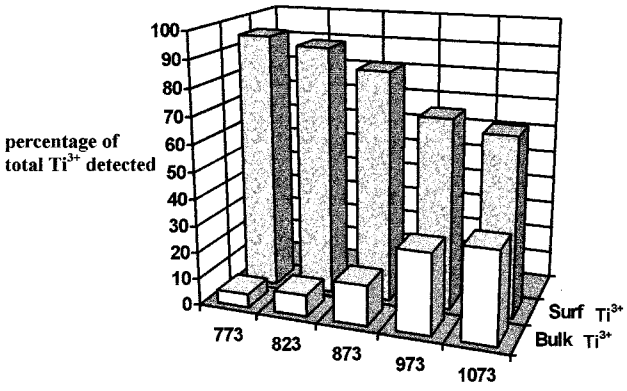

Figure 1. Variations in the ratio of surface-to-bulk Ti^{3+} composition in rutile TiO_2 as a function of the vacuum reduction temperature.

Preadsorption of Aldehydes and O_2. Prior to the study of the influence of coadsorbed oxygen/aldehyde gases on the interfacial photochemistry of thermally reduced TiO_2, the effects of preadsorption of the aldehyde or oxygen were individually investigated. Figure 2 shows the series of EPR spectra obtained after adsorption of acetaldehyde onto rutile TiO_2 that was thermally reduced at 823 K in vacuo (Figure 2a). After exposure of the sample to 1 Torr of acetaldehyde at 100 K, there was an increase in the intensity of the signal at $g = 2.0023$ associated with medium-polarized electrons (Figure 2b), which is indicative of adsorbate contact with the TiO_2 surface.[19,21] The simultaneous decrease in intensity of the Ti^{3+} resonance at $g = 1.962$ is caused by partial reoxidation of the TiO_2 by acetaldehyde. A minor peak at $g = 1.922$ is also observed and believed to arise from traces of a second bulk Ti^{3+} center but will not be discussed further in this paper.

Subsequent UV irradiation of the rutile material in the presence of acetaldehyde resulted in the appearance of a new set of resonances at $g = 2.043$, 2.029, and 2.026. These latter resonances can be assigned to trapped holes (O^- centers) in axial symmetry, as previously reported by others in TiO_2.[9,10,12,13] UV irradiation of the acetaldehyde-exposed material also caused a regrowth of the Ti^{3+} species, consistent with photoexcited conduction electrons becoming trapped at Ti^{3+} defect centers. Warming the irradiated rutile sample to 300 K followed by recooling to 100 K for EPR measurements resulted in the loss of all photoformed paramagnetic centers from the EPR spectrum.

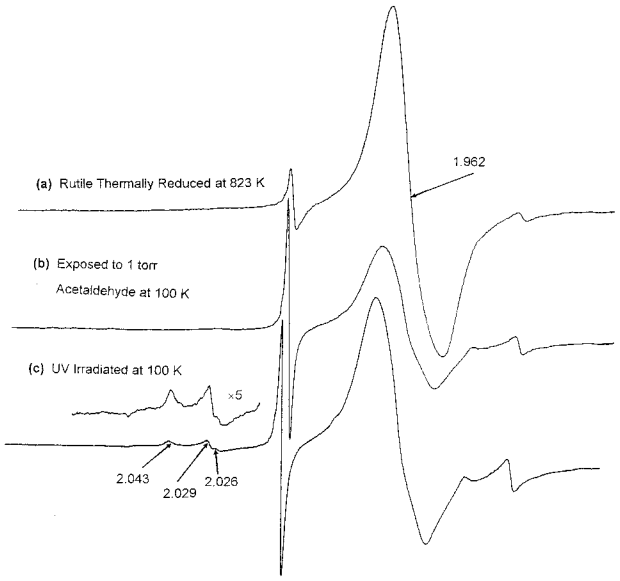

Figure 2. EPR spectra of (a) reduced TiO_2 (823 K), (b) after adsorption of 1 Torr of *acetaldehyde* at 77 K and warmed to 100 K, and (c) after subsequent UV irradiation at 100 K for 1 min.

However, all such centers could be restored by reirradiation of the sample at 100 K.

The general spectral responses shown in Figure 2 are also observed for preadsorbed formaldehyde and benzaldehyde on thermally reduced rutile TiO_2 (spectra not shown). It should be noted, however, that the relative spectral intensity changes accompanying adsorbate contact are slightly different for each aldehyde, owing to differences in their relative reduction potentials (with respect to the conduction band edge) and electrophilic character. However aldehyde-derived surface radicals were *not* observed in any of these preadsorption studies, irrespective of the aldehyde identity or extent of TiO_2 vacuum reduction. Subsequent adsorption of O_2 onto the reduced rutile TiO_2 containing the preadsorbed aldehyde, and prior to UV irradiation, produced similar spectral responses to those shown in Figure 2. No significant changes occurred in the spectrum.

The adsorption of O_2 onto reduced TiO_2 surfaces is a well-established method for the preparation of stable superoxide radical anions (O_2^-). The resulting EPR spectrum (not shown) is consistent with the presence of superoxide radicals stabilized on Ti^{4+} cations in orthorhombic symmetry.[25−28] After this sample was warmed to 300 K, followed by recooling to 100 K for EPR measurements, there was a slight increase in the O_2^- signal intensity. Furthermore, the O_2^- species in this case was found to be stable up to 400 K, decaying rapidly and irreversibly above this temperature. Subsequent exposure of the TiO_2 to aldehyde vapor, after preadsorption of O_2, does not produce any new EPR resonances, even when the system was irradiated at 100 K. The thermal stability of adsorbed superoxide was not affected by addition of the aldehydes or by irradiation at 100 K.

Coadsorption of Formaldehyde/O_2. Figure 3 shows the EPR spectrum obtained after UV irradiation at 100 K of TiO_2 (reduced at 723 K) containing coadsorbed formaldehyde/O_2 (10 Torr). The observed EPR signal was not found prior to UV irradiation. At first glance, the new signal appears to be characterized by two components at $g = 2.017$ and 2.008. However, closer inspection of the spectrum reveals a third component at $g \approx 2.003$ superimposed on the signal at $g = 2.0023$ because of the localized conduction band electrons (this third component is more evident in the presence of acetaldehyde

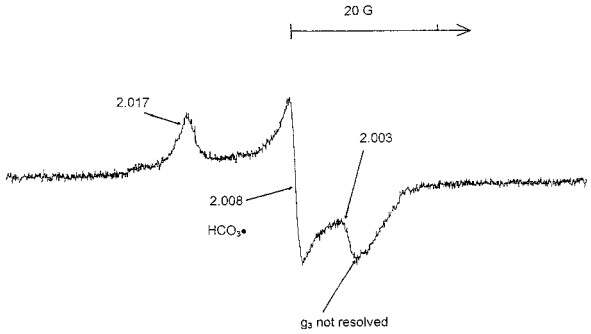

Figure 3. EPR spectrum (100 K) of the surface radicals (identified as HCO_3•) formed by UV irradiation at 100 K ($\lambda > 340$ nm) of coadsorbed *formaldehyde*/O_2 on the 723 K reduced TiO_2.

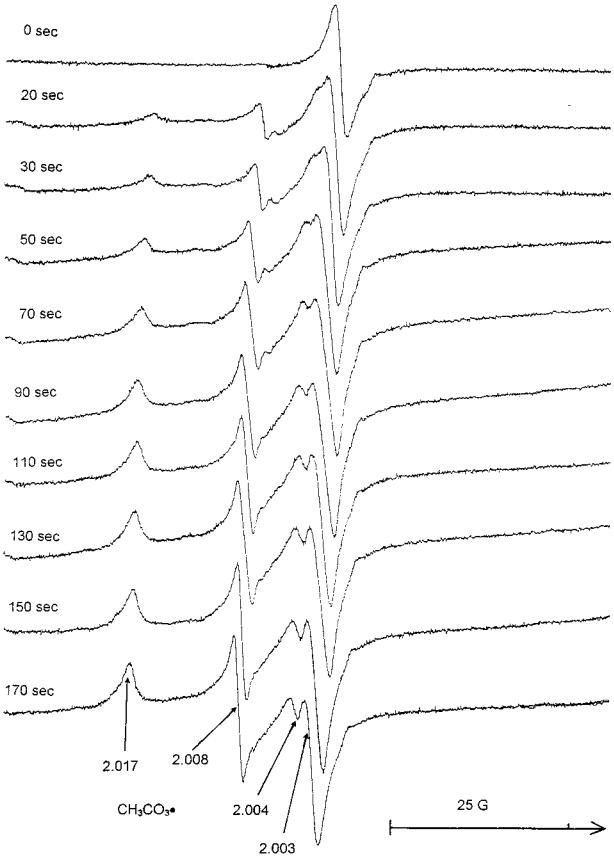

Figure 4. Evolution and growth of the new surface radical signal (identified at CH_3CO_3•) as a function of UV irradiation time at 100 K on TiO_2 (reduced at 773 K) containing coadsorbed *acetaldehyde*/O_2.

and benzaldehyde, as seen in and discussed for Figures 4 and 5 below). The paramagnetic species responsible for the new signal does not, however, display any clear hyperfine couplings (Table 1).

The possibility that the new spectrum arises from superoxide radicals can be immediately discounted, since the *g* values differ markedly from those of O_2^- on the same sample and since the new radical decays gradually with increasing temperature; its EPR spectrum is completely and irreversibly lost at $T > 250$ K, in contrast to O_2^-, which is stable at temperatures up to 400 K. Irradiation at 100 K using 340 and 380 nm UV cutoff filters produces the same radical signal in Figure 3, though the spectral intensity is observed to decrease with increasing UV wavelength. This loss in spectral intensity is most likely due to the attenuation of photon flux and intended loss in transmission of photons with energy much greater than the band gap threshold excitation, through the cutoff filters.

TABLE 1: EPR *g* Values for the Paramagnetic Centers Observed in This Work

paramagnetic species	*g* values		
	g_1	g_2	g_3
localized conduction electrons	$g_{iso} = 2.0023$		
Ti^{3+} defect centers: bulk and surface Ti^{3+}	$g_\perp = 1.962$; $g_\parallel = 1.949$		
trapped holes: O^- centers	$g_\perp = 2.026, 2.029, 2.043$; $g_\parallel = 2.00$		
superoxide anions: O_2^- centers	2.022	2.011	2.008
surface radicals: $RCO_3^\bullet$			
formaldehyde/$O_2 \rightarrow HCO_3^\bullet$	2.017	2.008	2.003
acetaldehyde/$O_2 \rightarrow CH_3CO_3^\bullet$	2.017	2.008	2.003
benzaldehyde/$O_2 \rightarrow C_6H_5CO_3^\bullet$	2.016	2.007	2.0017

Coadsorption of Acetaldehyde/O_2. Following the coadsorption of acetaldehyde/O_2 on rutile TiO_2 (reduced at 823 K in vacuo), the response of the polarized conduction electrons at $g = 2.0023$ and Ti^{3+} centers was similar to that described above in the preadsorption studies (Figure 2b). However, UV irradiation of the sample containing the coadsorbed gases leads to the generation of a new EPR signal (similar to Figure 3) and characterized by *g* values at 2.017 and 2.008. To determine whether the new surface signal formed from coadsorbed acetaldehyde/O_2 displays axial or orthorhombic symmetry, the experiment was repeated using rutile TiO_2 reduced in vacuo at the lower temperature of 773 K. The resulting series of EPR spectra, showing radical growth versus irradiation time, is shown in Figure 4. The lower level of medium polarization in the 773 K activated material allows clear identification of an additional resonance at $g = 2.004$, which was obscured by the larger $g = 2.003$ signal on the 823 K reduced material. As in the case of formaldehyde/O_2 coadsorption, the surface radical observed in acetaldehyde/O_2 studies decayed irreversibly at $T = 250$ K and was also generated by irradiation with light of $\lambda > 380$ nm.

Coadsorption of Benzaldehyde/O_2. Benzaldehyde was chosen as the subject for aromatic aldehyde coadsorption studies for several important reasons. First, benzaldehyde is the simplest of the aromatic aldehydes and its moderate vapor pressure (1 mm Hg at 300 K) allows for greater ease of handling and pressure control under vacuum. Second, it was hoped that resonance-stabilized benzaldehyde-derived radicals would provide more intense surface radical spectra.

Figure 5 shows a series of EPR spectra obtained from coadsorption and subsequent UV irradiation of benzaldehyde (10 Torr) with O_2 on rutile TiO_2 (reduced at 723 K in vacuo). Altering the O_2 pressure in the range 1−10 Torr had no effect on the recorded EPR spectrum. The orthorhombic EPR signal that developed following UV irradiation was consistent with a surface radical species. The appearance of several overlapping resonances was also suggestive of the presence of more than one such surface species. EPR resonances associated with trapped holes were also evident following irradiation and were significantly broadened with increasing irradiation time. The surface radical species detected from benzaldehyde (10 Torr)/O_2 (1 Torr) coadsorption decayed irreversibly above $T = 250$ K but was also generated by irradiation at $\lambda > 380$ nm.

Figure 6 shows the EPR spectra obtained from coadsorption and irradiation of 1 Torr of benzaldehyde with O_2 on rutile TiO_2 reduced at 723 K in vacuo. Once again, altering the O_2 pressure in the range 1−10 Torr had no effect upon the recorded EPR spectrum. The surface radical signal observed following irradiation using 1 Torr of benzaldehyde, however, displayed two distinct resonances at $g = 2.018$ and 2.0166, which were not independently resolved in the presence of higher benzaldelyde pressures (10 Torr) (Figure 5).

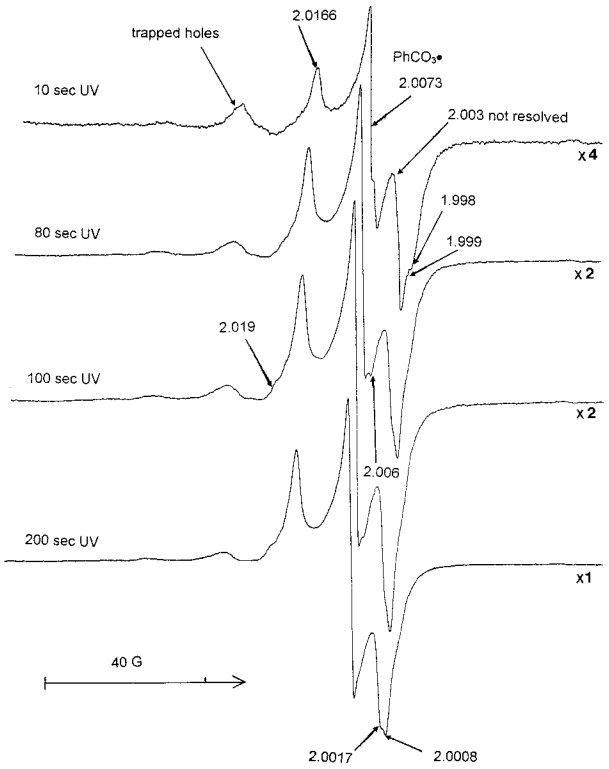

Figure 5. Spectra of new surface radical (identified as $C_6H_5CO_3^\bullet$) as a function of UV irradiation time (from 10 to 200s) at 100 K on TiO_2 (reduced at 723 K) containing coadsorbed *benzaldehyde*/O_2 (10 Torr).

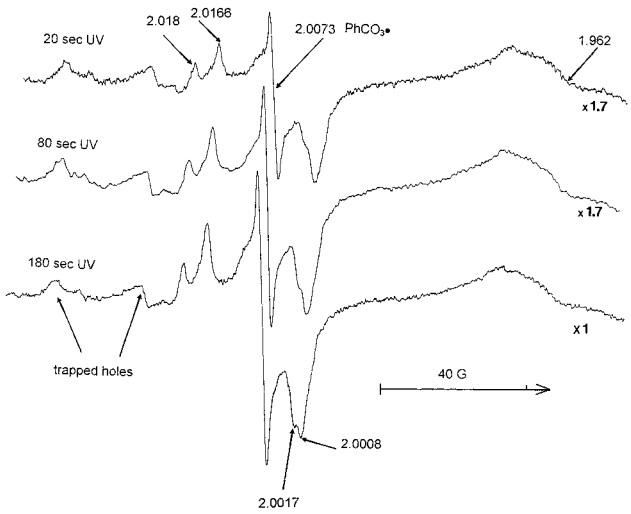

Figure 6. Changes in the EPR spectra of $C_6H_5CO_3^\bullet$ as a function of UV irradiation time (20−180s) at 100 K on TiO_2 (reduced at 723 K) containing coadsorbed *benzaldehyde*/O_2 (1 Torr).

Irradiated Suspensions. To ensure that the exposure of TiO_2 powders to aldehyde vapor pressures of 1−10 Torr did not result in the formation of aldehyde "ices", rutile TiO_2−aldehyde suspensions were also UV-irradiated at 100 K. The irradiation of neat benzaldehyde at 100 K led to the production of an EPR signal with $g = 2.002$, consistent with a carbon-centered radical located in an "ice" matrix. This radical spectrum displayed no evidence for a nuclear hyperfine coupling, was not affected by oxygenation of the suspension, and was stable up to 150 K. Irradiation of the rutile TiO_2−benzaldehyde suspension also resulted in the production of a structureless organic radical resonance at $g = 2.002$ in addition to a strong Ti^{3+} signal at $g = 1.962$. Oxygenation of the suspension prior to irradiation had

the effect of reducing the Ti^{3+} signal intensity but did not alter the characteristics of the organic species detected.

Discussion

Effects of Thermal Reduction of Rutile TiO_2 in Vacuo. The response of rutile TiO_2 to reduction in vacuo at various temperatures was measured in order to determine the optimum temperature of reduction for solid−gas interface studies. At 723 K, no Ti^{3+} signal develops and only medium-polarized electrons are detected. Above 723 K, reduction of TiO_2 is observed, as evidenced by the increase in intensity of the Ti^{3+} signal at g = 1.962. This signal has been reported previously[9,10] and has been assigned to a composite resonance arising from both surface and bulk Ti^{3+} centers formed via O_2 loss from the oxide surface during thermal reduction under vacuum:

$$2O^{2-}_{(latt)} \rightarrow O_{2(g)} + 4e^- \quad (1)$$

$$4Ti^{4+} + 4e^- \rightarrow 4Ti^{3+} \quad (2)$$

As the reduction temperature is increased, the proportion of Ti^{3+} centers formed in the oxide bulk increases as a fraction of the total Ti^{3+} signal (Figure 1). Above 823 K, the ratio of surface-to-bulk Ti^{3+} begins to decrease rapidly so that reduction at $T > 823$ K only produces extensive bulk reduction, since the surface region is fully reduced. Thus, reduction above this temperature simply produces a large bulk Ti^{3+} resonance at $g = 1.962$, which will obscure the EPR signals of any surface radical.

The findings that higher reduction temperatures cause an increase in bulk TiO_2 reduction is in agreement with the recent results of Henderson,[29] who studied the reoxidation of TiO_2 surfaces by a diffusion mechanism involving Ti^{3+} mass transfer between the surface and the bulk of the oxide. However, he suggested that the majority of bulk reduction occurs via a defect transport mechanism involving diffusion of interstitial Ti^{3+} cations above 700 K. Although our results are in partial agreement with this assertion (since enhanced levels of interstitial Ti^{3+} cations[9] at $g = 1.99$ were observed at higher reduction temperatures), most of the bulk Ti^{3+} centers are clearly not located in interstitial sites. One explaination for this may be due to the method of abrasive milling used to prepare the high surface area rutile material used in this study. The abrasion of rutile surfaces is known to result in a high number of surface dislocations and stacking faults that close off the open *c*-axis interstitial diffusion channels of the rutile structure, leading to lower diffusion coefficients for interstitial ion mass transport between the surface and bulk.[30]

Behavior of Trapped Charge Carriers at the Illuminated TiO_2 Interface. Exposure of the TiO_2 surface to aldehyde vapor has two noticeable effects on trapped charge carrier states (Figure 2). First, the reduction in intensity of Ti^{3+} centers is indicative of charge transfer from surface Ti^{3+} sites to adsorbed aldehyde. However, at 100 K, this process does not result in the formation of stable surface anion radicals for any of the aldehydes studied, most probably because of radical anion fragmentation (or reaction) at this temperature. Electron transfer from the surface to the adsorbed aldehydes is expected to result in population of the lowest unoccupied π^*_{CO} molecular orbital (population of which results in wavelength-dependent aldehyde fragmentation in photoinitiated Norrish-type processes) so that C−C or C−H bond cleavage is expected. Radical ion cleavage has been previously reported for carbon−carbon bond formation reactions over illuminated TiO_2,[31] thus preventing back electron transfer, which would otherwise retard the rate of photocatalytic reaction. Second, contact of the aldehyde with the TiO_2 surface also results in an increased level of medium polarization of conduction electron states at $g = 2.003$. Naccache et al.[20] attributed this response to polarization of conduction electron states by surface electrophilic adsorbates, although the precise mechanism for stabilization of medium polarization remains unclear.[21] The presence of such states prior to adsorbate contact (following reduction in vacuo) is generally attributed to medium polarization via intrinsic surface and bulk impurity defects.[19]

Irradiation of the aldehyde-exposed TiO_2 at 100 K also results in the appearance of new EPR signals with multiple g components at $g_\perp = 2.026$, 2.029, and 2.043 having a common $g_{||}$ component at $g = 2.0020$. Similar resonances have been reported previously in TiO_2 and were assigned to trapped hole states O^-.[10,12,13,32] Irradiation of the aldehyde-exposed TiO_2 also leads to repopulation of Ti^{3+} states that became oxidized to Ti^{4+} on aldehyde contact, as evidenced by the regrowth of the Ti^{3+} signal at $g = 1.962$. However, when the sample is heated to 300 K, these photogenerated Ti^{3+} centers are once again reoxidized to Ti^{4+}, indicating that not all of the adsorbed aldehyde is reduced on initial contact with the TiO_2 surface at 100 K; Ti^{3+} centers formed by vacuum reduction are stable at 300 K in vacuo prior to the addition of aldehyde. All O^- centers are also completely lost on warming the sample to 300 K. Since the total spectral intensity of photogenerated holes is much lower than that of photogenerated Ti^{3+}, not all of the Ti^{3+} reoxidation can be accounted for by electron−hole recombination, and a proportion must be due to reaction with adsorbed aldehyde. The irradiation−warm−recool cycle can be repeated several times before significant signal intensity losses are encountered, most probably due to depletion of adsorbed aldehyde via surface reaction. The aldehyde identity has no effect upon the EPR spectral characteristics of any of the trapped charge carriers observed in preadsorption studies.

It is notable that the distribution of observed trapped charge carriers is markedly different in irradiated frozen suspensions when compared to gas−solid studies. Most striking is the complete absence of trapped holes from the EPR spectra obtained from irradiation of frozen rutile TiO_2−aldehyde suspensions. Recently, Ishibashi et al.[33] have reported that the "deactivation" of trapped holes on TiO_2 proceeds very rapidly in the presence of adsorbed organics. The rate of this reaction is expected to be directly proportional to the surface coverage of organics, which is greatly in excess of one monolayer for frozen suspensions. However, for exposure of TiO_2 to low aldehyde vapor pressures (less than 1 Torr at 100 K), the surface coverage is possibly below one monolayer. Moreover, even if the surface coverage did exceed one monolayer, the supply of aldehydes (or their reaction products) to reactive surface centers such as O^- would deplete much more quickly during the course of irradiation for the lower coverage gas−solid interface.

It is also noteworthy that O^- centers are not observed during the course of UV irradiation of rutile surfaces predosed with O_2, even though large quantities of O_2^- are generated via electron transfer from TiO_2 to adsorbed O_2. The O_2^- species present on the TiO_2 surface clearly originate from gaseous O_2, since the surface is well dehydroxylated prior to O_2 admission and O_2^- anions formed both via adsorption and irradiation are stable up to 400 K. Since irradiation at 100 K clearly leads to the formation of valence band holes and conduction band electrons, the question arises as to the mechanism of hole deactivation on the O_2-exposed material. Howe and Gratzel[10] have suggested that irradiative loss of O_2^- may be due to

oxidation by holes, or reduction by electrons, on the hydroxylated surface at 77 K:

$$O_2^- + h^+ \rightarrow O_2 \quad (3)$$

$$O_2^- + e^- \rightarrow O_2^{2-} \quad (4)$$

Moreover, the moderate growth in intensity of the O_2^- signal in the case of the dehydroxylated material was accompanied by a simultaneous increase in the intensity of the Ti^{3+} signal at $g = 1.962$, thereby suggesting oxidation of adsorbed superoxide as the possible major pathway. Evidence for the deactivation of holes (as $OH^\bullet$, O^-, or "free" h^+) via reaction with O_2^- has also recently been provided by Ishibashi et al.[33] and can only be rationalized for direct reaction of O_2^- with itinerant holes or O^- in the system studied here. Furthermore, the stability of the O_2^- signal observed during the course of irradiation in this case is most likely due to dynamic equilibrium between O_2^- photoformation and oxidative loss in the absence of surface OH functions.

Nature of the Surface Radical Species (F) on Irradiated TiO_2. The free radical mechanism of aldehyde oxidation is well-known[22] and is initiated by H atom abstraction via reaction with a valence band hole in TiO_2-mediated photocatalysis (eq 5):

$$RCHO + h^+ \rightarrow RCO^\bullet \quad (5)$$

$$RCO^\bullet + O_2 \rightarrow RCO_3^\bullet \quad (6)$$

$$RCO_3^\bullet \rightarrow RCO_3H + RCO^\bullet \quad (7)$$

$$RCO_3H + RCHO \rightarrow 2CH_3(CO)OH \quad (8)$$

Equations 5−8 represent an idealized reaction scheme in which several possible side reactions of the $RCO_3^\bullet$ radical are omitted for clarity, e.g., dimerization to form an unstable tetraoxide intermediate.[34] Following the initial $H^\bullet$ abstraction step to form an acyl-type radical, the oxidation proceeds via the chain reaction sequence shown in eqs 6−8. However, the extent to which the TiO_2 surface participates in the chain reaction sequence has not been fully ascertained in the current literature. Recently, Ohko et al.[34] have proposed that radical chain reactions do not proceed to a significant extent on the hydroxylated TiO_2 surface for acetaldehyde oxidation at moderate UV intensities. They also report that high rates of termination reactions are favored by high concentrations of radical species, which would account for the failure to detect the $RCO_3^\bullet$ species in frozen suspensions of either hydroxylated or dehydroxylated TiO_2 in this study.

The radical species detected in frozen suspensions of acetaldehyde and benzaldehyde (characterized by the isotropic g value at $g = 2.002$) displayed no evidence of hyperfine coupling to aldehydic hydrogens and can be generated by photolysis of deoxygenated solutions, both in the presence and absence of TiO_2. It thus seems likely that these species are formed via primary dissociation of the aldehyde by a Norrish-type dissociation in which semiconductor-derived holes or electrons do not participate.[18] The lack of an observable hyperfine structure in these radicals suggests that they are stable acyl species ($RCO^\bullet$) located in the frozen aldehyde matrix. The $H^\bullet$ atom species formed from such C−H bond dissociations would be highly reactive at 100 K and in fact are only detectable by EPR at temperatures well below 50 K.[35] The failure to detect acyl species at the gas−solid interface (for both hydroxylated and dehydroxylated TiO_2) for the lowest aldehyde vapor pressure studied (1 Torr) suggests that these species are not easily stabilized on the TiO_2 surface. However, acetaldehyde-derived acyl and carboxyl radicals have been detected desorbing from hydroxylated rutile TiO_2 surfaces by the spin-trapping EPR method,[36] indicating that they are formed as short-lived intermediates at the TiO_2−liquid interface in the heterogeneous photodegradation of aldehydes.

The coadsorption of aldehydes and O_2 onto the reduced rutile surface does not initially result in the production of stable surface radical species, even though reoxidation of the TiO_2 surface via loss of Ti^{3+} centers is observed. However, irradiation of this surface does result in the formation of a new stable surface radical species at 100 K. The orthorhombic **g** tensor values observed for this species are different from those observed for O_2^- on the same rutile material, and the new species undergoes an irreversible decay at ca. 250 K for all aldehydes studied. Furthermore, preadsorption of O_2 (yielding O_2^-, which is stable up to 400 K) followed by adsorption of aldehydes results only in the production of stable superoxide even when the system is irradiated at 100 K. Moreover, the concentration of surface radicals obtained in the coadsorption studies is observed to vary in direct proportion to the aldehyde vapor pressure when the O_2 pressure is held constant, suggesting that these species are of aldehydic origin. The approximate doubling of surface radical signal intensity on doubling the aldehyde vapor pressure suggests that the radical formation process is approximately first order with respect to aldehyde concentration. Given that no hydrogen hyperfine splitting is observed in the case of coadsorbed formaldehyde/O_2, the $RCO^\bullet$ radical is ruled out as a possible candidate (R = H for formaldehyde). Should stable formyl radical formation result from the $H^\bullet$ abstraction from formaldehyde during the course of UV irradiation (eq 5), then an EPR spectrum with a hydrogen hyperfine coupling of 130 G should be observed.[37]

The rate of photoformation of surface radicals generated from coadsorption is slow when compared to O_2^- formation, requiring ca. 170−200 s to reach a maximum concentration for the former and only 15−20 s for the latter. This is suggestive of a slow diffusion-controlled process leading to the formation of surface radicals. Since both electron and hole trapping are fast processes at the TiO_2 surface (ca. 10 ns for holes and 100 ps for electrons),[38] the slow accumulation of surface radicals under UV irradiation is thought to arise as a consequence of reactant diffusion over the TiO_2 surface. Although ionic species such as O_2^- are effectively immobilized on metal oxide surfaces at 100 K, the neutral aldehyde and O_2 molecules will possess some mobility at this temperature. It is thus deduced that the surface radical species formed from irradiation of coadsorbed aldehyde/O_2 is the peroxyacyl radical $RCO_3^\bullet$. The stability of peroxyl-type radicals is known to be highly sensitive to the terminal oxygen spin density, which is relatively low in the peroxyacyl species because of the proximity of the electrophilic carbonyl function. Stable methylperoxy[39] and propylperoxy[40] species have been observed by EPR at 100 K on MgO and Bi_2O_3, respectively, and terminal oxygen spin densities have been measured in the range $\rho_\pi = 0.70-0.61$.[41] Since most of the unpaired spin density is associated with the terminal peroxy oxygen, this accounts for the absence of any hyperfine interaction with the protons of the R group. Sevilla et al.[41] have conducted an extensive study of carbon-based peroxyl radicals, with g values varying only slightly from $g_1 = 2.035$, $g_2 = 2.008$, and $g_3 = 2.003$; the greatest deviation was found for the crystal-field-sensitive g_1 component.

To our knowledge, the only stable surface peroxacyl radical reported previously was generated via biacetyl decomposition in the presence of acetaldehyde and O_2 over KCl-modified SiO_2, which also displayed an orthorhombic **g** tensor system with $g_1 = 2.025$, $g_2 = 2.005$, and $g_3 = 2.002$.[42] The possibility that the $RCO_3^\bullet$ species might decay to produce $RCO_2^\bullet$ via tetraoxide decomposition or that any RCO_3H formed might decay via the previously reported reaction[43]

$$RCO_3H + Ti^{3+} \rightarrow Ti^{4+} + RCO_2^\bullet + OH^- \qquad (9)$$

was discounted for several reasons. First, carboxyl-type radicals possess significant spin density at the R position[41] so that hydrogen hyperfine couplings should be observable for the $HCO_2^\bullet$ radical at X-band EPR frequencies. Second, the molecular geometry of alkylcarboxyl radicals allows for rapid decarboxylation (producing CO_2 plus alkyl radicals) in UV light, and such species do not persist for longer than ca. 1 μs in the absence of stabilizing reactions such as H atom abstraction by the carboxyl radical to yield a carboxylic acid.[44] Furthermore, previous studies of amino acid photoadsorption at TiO_2 surfaces in frozen suspensions have yielded axial ($2g$ value) EPR resonances for $RCO_2^\bullet$ species formed via hole "trapping" at the amino acid carboxyl function.[14]

The persistence of the $RCO_3^\bullet$ radicals under continuous UV irradiation may be a contributory factor in the well-known phenomenon of dark recovery of photocatalytic activity over TiO_2 particles. The use of periodic irradiation is believed to increase the overall photocatalytic efficiency via "surface relaxation", in which photostable surface species, which retard the rate of interfacial charge transfer or participate in nonproductive side reactions, are believed to decay during the dark period.[45] However, since no peroxyacyl radicals are detected from coadsorption on the hydroxylated surface, recovery processes involving the decay of organic intermediates are probably more important in nonaqueous photocatalytic systems where the TiO_2 surface is depleted of hydroxyl functions. The failure to detect peroxyacyl species on the hydroxylated rutile surface is attributed to a high rate of termination processes, mediated via the coupling of species such as $OH^\bullet$ and O_2 to form reactive intermediates such as $HO_2^\bullet$.[46] The reaction of $HO_2^\bullet$ radicals with $RCO_3^\bullet$ species is believed to account for a significant proportion of termination reactions in the photooxidation of aldehydes over TiO_2, resulting in the formation of peroxoacids plus O_2.[47]

Mechanistic Considerations of $RCO_3^\bullet$ Formation. Despite the highly efficient electron-scavenging behavior of adsorbed O_2, no O_2^- radicals are observed on the irradiated TiO_2 surface coadsorbed with aldehydes/O_2. Indeed, electron transfer to dioxygen forming O_2^- is required as the reduction half-step for sustained aldehyde photooxidation to carboxylic acids, a functional group transformation in which O_2^- does not participate.[18] This raises the question of the fate of O_2^- on the TiO_2 surface for an overall reaction in which superoxide is produced but apparently not consumed. The presence of adsorbed aldehyde thus seems to have an inhibitory effect on stable superoxide formation on the rutile surface under UV illumination at 100 K. However, this is rather surprising given that superoxide is known to be very stable on dehydroxylated TiO_2 surfaces in this temperature regime.[48] However, during the course of UV irradiation, hole transfer to the aldehyde must result in some degree of "rehydroxylation" of the TiO_2 surface via H atom transfer to surface holes. Stable O_2^- may then become difficult to form, since photoinitiated radical addition reactions of superoxide at hydrated and partially hydrated TiO_2 surfaces are known to destabilize adsorbed superoxide at 77−100 K.[49] Also, since the rate of hole transfer is believed to be much faster than the rate of electron transfer across the interface (ca. 100 ns versus several milliseconds, respectively),[38] reaction with $RCO^\bullet$ radicals may be kinetically favored over O_2^- formation for a proportion of adsorbed O_2 molecules. The oxidation of the aldehydes may thus be written

$$RCHO_{ads} + TiO^-_{surf} \rightarrow RCO^\bullet_{ads} + TiOH^-_{surf} \qquad (10)$$

$$RCO^\bullet_{ads} + O_{2\,ads} \rightarrow RCO_3^\bullet \qquad (11)$$

It should be remembered that the inability to observe stable acyl radicals during the course of aldehyde oxidation is probably due to their high reactivity toward molecular oxygen and other radical species rather than to dissociative loss. Acyl radicals are σ radicals with the unpaired electron density located primarily in an sp hybrid orbital of the carbonyl carbon,[50] and thus, they undergo rapid radical addition reactions. However, unlike the $RCHO^\bullet$ intermediates formed during aldehyde reduction on TiO_2, they do not possess any significant antibonding orbital occupation and are not expected to decompose by intramolecular dissociation.

Furthermore, although the superoxide does not participate in the main oxidative pathway of aldehydes, the complete conversion of aldehydes to CO_2 is known to proceed via the intermediacy of carboxylic acid oxidation,[18] a reaction in which the superoxide does participate. Thus, under prolonged and intense UV irradiation (which is known to promote carboxylic acid formation via tetraoxide decomposition),[34] O_2^- may be consumed in secondary oxidation reactions. However, the precise mechanism of superoxide destabilization in coadsorption studies remains somewhat speculative at this time.

Conclusions

The thermal activation characteristics of the rutile TiO_2 used in this study were studied by EPR spectroscopy. Vacuum reduction results in the formation of localized conduction electrons and Ti^{3+} centers in both bulk and surface sites. By use of O_2 to preferentially remove surface Ti^{3+} centers, EPR spectra of bulk and subsurface Ti^{3+} cations can be obtained. The increase in bulk Ti^{3+} concentrations with increasing activation temperature is consistent with studies by other authors, indicating cationic mass transfer between the surface and subsurface in a vacuum-reduced rutile.

Adsorption of aldehydes onto the reduced surface at 100 K causes immediate oxidation of the Ti^{3+} centers, but no stable surface paramagnetic species are formed. Medium polarization of conduction electrons is also observed, providing firm evidence for substrate contact with the TiO_2 surface. Subsequent UV irradiation of the aldehyde-doped TiO_2 does not lead to paramagnetic radical formation despite evidence for band gap mediated photocatalysis. The failure to detect paramagnetic surface intermediates under these conditions is attributed to surface-mediated radical recombination processes.

By coadsorption of aldehydes and oxygen, as opposed to successive preadsorption steps, new surface radical species have been identified on the dehydroxylated TiO_2 surface. By analysis of the g values of these radicals and comparision of the stabilities with those of superoxide anions formed under similar conditions, the results of aldehyde/O_2 coadsorption studies provides strong evidence for the formation of stable surface oxidative intermediates at 100 K on rutile TiO_2. Variable wavelength studies indicate that these intermediates are formed by band gap

mediated electronic excitatations and not by direct excitation of the aldehyde to form Norrish-type photodissociation products. The surface radical species were assigned to peroxyacyl species ($RCO_3^{\bullet}$), which are known oxidative intermediates in the autocatalytic oxidation of aldehydes. The peroxyacyl reactive intermediates are only formed under coadsorption conditions; predosing the reduced surface with aldehyde followed by O_2, or vice versa, will not produce the $RCO_3^{\bullet}$ species. Strict attention must therefore be given to the possible different reaction pathways that accompany consecutive adsorption as opposed to coadsorption methods in heterogeneous photocatalysis.

Acknowledgment. Funding from EPSRC and ICI Tioxide is gratefully acknowledged.

References and Notes

(1) Heller, A.; Broch, J. R. Materials and Methods for Photocatalyzing Oxidation of Organic Compounds on Water. U.S. Patent 4-997-576, March 1991.
(2) Sakai, H.; Baba, R.; Hashimoto, K.; Kubota, Y. *Chem. Lett. Jpn*. **1995**, *3* 185.
(3) *Solar Detox Update*; National Renewable Energy Laboratory, U.S. Department of Energy: Boulder, CO, 1994; Volume 1, No. 1, p 1.
(4) Ferry, J. L.; Glaze, W. H. *J. Phys. Chem. B* **1998**, *102*, 2239.
(5) Idriss, H.; Kim, K. S.; Barteau, M. A. *Surf. Sci*. **1992**, *262*, 113.
(6) Cain, S. R.; Emmi, F. *Surf. Sci.* **1990**, *232*, 209.
(7) Busca, G.; Lamotte, J.; Lavalley, J. C.; Lorenzelli, J. *J. Am. Chem. Soc.* **1987**, *109*, 5197.
(8) Bates, S. P.; Gillan, M. J.; Kresse, G. *J. Phys. Chem. B* **1998**, *102*, 2017.
(9) Howe, R. F.; Gratzel, M. *J. Phys. Chem.* **1985**, *89*, 4495.
(10) Howe, R. F.; Gratzel, M. *J. Phys. Chem*. **1987**, *91*, 3906.
(11) Anpo, M.; Shima, T.; Kubokawa, Y. *Chem. Lett.* **1985**, 1799.
(12) Micic, O. I.; Zhang, Y.; Cromack, K. R.; Trifunac, A. D.; Thurnauer, M. C. *J. Phys. Chem.* **1993**, *97*, 7277.
(13) Micic, O. I.; Zhang, Y.; Cromack, K. R.; Trifunac, A. D.; Thurnauer, M. C. *J. Phys. Chem.* **1993**, *97*, 13284.
(14) Rajh, T.; Ostafin, A. E.; Micic, O. I.; Tiede, D. M.; Thurnauer, M. C. *J. Phys. Chem.* **1996**, *100*, 4538.
(15) Nosaka, Y.; Koenuma, K.; Ushida, K.; Kira, A. *Langmuir* **1996**, *12*, 736.
(16) Gray, T. G.; McCain, C. C.; Masse, N. G. *J. Phys. Chem.* **1959**, *63*, 472.
(17) Iyengar, R. D.; Codell, M.; Kara, J.; Turkevitch, J. *J. Am. Chem. Soc.* **1966**, *88*, 5055.
(18) Schwitzgebel, J.; Ekerdt, J. G.; Gerischer, H.; Heller, A. *J. Phys. Chem.* **1995**, *99*, 5633.
(19) Ismagilov, Z. R.; Pak, S. N.; Yermolaev, V. K. *J. Catal.* **1992**, *136*, 197.
(20) Naccache, C.; Meriadeau, P.; Che, M.; Tench, A. J. *Trans. Faraday Soc.* **1971**, *67*, 506.
(21) Serwicka, E.; Schlierkamp, M. W.; Schindler, R. N. *Z. Naturforsch.* **1981**, *36a*, 226.
(22) Clinton, N. A.; Kenley, R. A.; Traylor, T. G. *J. Am. Chem. Soc.* **1975**, *97*, 3746.
(23) Grosser, E.; Baunok, I. *S. Afri. J. Sci.* **1992**, *88*, 375.
(24) Leonardos, G.; Kendall, D.; Barnard, N. *J. Air Pollut. Control. Assoc*. **1969**, *19*, 91.
(25) Anpo, M.; Aikawa, Y.; Kubokawa, M.; Che, M.; Louis, C.; Giamello, E. *J. Phys. Chem.* **1985**, *89*, 5689.
(26) Shvets, V. A.; Kazansky, V. B. *J. Catal*. **1972**, *25*, 123.
(27) Shiotani, M.; Moro, G.; Freed, J. H. *J. Chem. Phys*. **1981**, *74*, 2616.
(28) Murphy, D. M.; Griffiths, E. W.; Rowlands, C. C.; Hancock, F. E.; Giamello, E. *J. Chem. Soc., Chem. Commun.* **1997**, 2177.
(29) Henderson, M. A. *Surf. Sci*. **1995**, *343*, L1156.
(30) Johnson, O. W. *Phys. Rev.* **1964**, *136*, A284.
(31) Cermenati, L.; Richter, C.; Albini, A. *J. Chem. Soc., Chem. Commun*. **1998**, *7*, 805.
(32) Zwingwl, D. *Solid State Commun*. **1976**, *20*, 397.
(33) Ishibashi, K.; Nosaka, Y.; Hashimoto, K.; Fujishima, A. *J. Phys. Chem. B* **1998**, *102*, 2117.
(34) Ohko, Y.; Tryk, D. A.; Hashimoto, K.; Fujishima, A. *J. Phys. Chem. B* **1998**, *102*, 2699.
(35) Reiderer, H.; Huttermann, J.; Boon, P.; Symons, M. C. R. *J. Magn. Reson.* **1983**, *54*, 54.
(36) Jenkins, C. A.; Murphy, D. M.; Rowlands, C. C.; Egerton, T. A. *J. Chem. Soc., Perkin Trans.* **1997**, *2*, 2479.
(37) Paul, H.; Fischer, H. *Helv. Chim. Acta* **1973**, *56*, 1575.
(38) Martin, S. T.; Hermann, H.; Choi, W.; Hoffmann, M. R. *Trans. Faraday Soc.* **1994**, *90*, 3315.
(39) Ito, T.; Wang, J. X.; Lin, C. H.; Lunsford, J. H. *J. Am. Chem. Soc.* **1985**, *107*, 5062.
(40) Driscoll, D. J.; Campbell, K. D.; Lunsford, J. H. *Adv. Catal*. **1987**, *35*, 139.
(41) Sevilla, M. D.; Becker, D.; Yan, M. *J. Chem. Soc., Faraday Trans.* **1990**, *86*, 3279.
(42) Bakhchaddjyan, R. H.; Vardanyan, I. A. *Int. J. Chem. Kinet*. **1994**, *26*, 595.
(43) Bawn, C. E. H.; Williamson, J. B. *Trans. Faraday Soc*. **1951**, *47*, 735.
(44) Edge, D. J.; Kochi, J. K. *J. Am. Chem. Soc*. **1973**, *95*, 2635.
(45) Sczechowski, J. G.; Koval, C. A.; Noble, R. D. *J. Photochem. Photobiol. A* **1993**, *74*, 273.
(46) Lu, G.; Linsebigler, A.; Yates, J. T., Jr. *J. Phys. Chem*. **1995**, *99*, 7626.
(47) Schuchumann, M. N.; Sonntag, C. V. J. *J. Phys. Chem.* **1979**, *83*, 780.
(48) Meriadeau, P.; Vedrine, J. C. *J. Chem. Soc., Faraday Trans. 2* **1976**, *72*, 472.
(49) Gonzalez-Elipe, A. R.; Munuera, G.; Soria, J. *J. Chem. Soc., Faraday Trans. 1* **1979**, *75*, 748.
(50) Bennet, J. E.; Mile, B. *Trans. Farday Soc.* **1971**, *67*, 1587.